An optical fibre pressure sensor

J.P. Dakin, C.A. Wade, P.B. Withers

Plessey Research Roke Manor Limited, Romsey, Hampshire, SO51 0ZN, U.K.

Abstract

The design, construction and testing of a fibre optic pressure sensor based on a reflecting Fabry-Perot etalon is described. The etalon comprised one fixed mirror and a second mirror designed to flex under the action of the pressure being monitored. A single multimode fibre was used to connect the passive, remote sensor to the transmitter/receiver section, and dual wavelength referencing was used to eliminate the effects of bending-induced attenuation in the fibre.

Introduction

The potential advantages of fibre optic sensors over conventional types are well known and include: immunity to electromagnetic interference; intrinsic safety in hazardous environments due to their electrically passive nature; and the convenience of remote sensing over low attenuation optical fibre.

The work described here was aimed at demonstrating a simple and rugged fibre optic sensor for the remote measurement of pressure. For high reliability, and to avoid potential inaccuracy due to hysteresis or backlash, the technique used was based on a Fabry-Perot etalon, in which the only movement during operation is a minute flexing of a silica plate under the action of the pressure to be measured. This technique has several additional attractions, such as requiring only a single multimode fibre connection and an ability to withstand large over- pressures without damage. Dual wavelength referencing was used to eliminate the effects of bending-induced attenuation in the fibre. The principle of operation, and the construction and testing of an experimental prototype are described in the following sections.

Principle of operation

The Fabry-Perot etalon comprises two plane, parallel reflectors as shown in figure 1a. The combination can be considered to be a compound mirror whose transmission and reflectivity depend on the wavelength of the incident radiation, the separation of the mirrors and their individual reflectivities.

Assuming that no energy is absorbed by the mirrors and that they are illuminated by a single frequency source, the intensities of the transmitted and reflected beams are given by I_t and I_r respectively, where from standard texts:

$$I_t = I_i \left(1 + F \sin^2 \left(\frac{2\pi n d \nu}{c} + \theta\right)\right)^{-1}$$

$$I_r = I_i - I_t$$

- d = mirror separation
- ν = frequency of source ($=c/\lambda$)
- n = refractive index of material between the mirrors
- θ = phase change occurring when light reflects off the mirrors, inside the cavity
- I_i = incident illumination intensity
- F = $4R/(1-R)^2$ where R = reflectivity of individual mirrors

The functions are depicted graphically in figure 1b, for a monochromatic source. Whereas the width of the peaks depends only upon R, their positions depend on the wavelength of the incident radiation and also on the mirror separation. As the mirror spacing changes, the intensities of the reflected and transmitted light pass through a series of maxima and minima, one complete cycle occurring when the spacing varies by $\lambda/2$, where λ is the wavelength of the incident illumination.

The mirrors will, in fact, absorb some of the incident light, and the optical source will have a finite spectral width. These departures from the ideal will decrease the modulation depth of the functions shown in the diagram.

In this application the etalon is designed so that the mirror separation is pressure sensitive: as the ambient pressure varies, the optical transmittance and reflectance of the device, at any specific wavelength, changes.

The Fabry Perot conveniently lends itself to a reflective configuration, in which the pressure to be sensed bears directly on the exposed mirror substrate, as shown in Figure 2. The pressure causes a minute deflection of the mirror substrate (directly proportional to the pressure), which can be detected by monitoring the intensity of the back-reflected light. This is reasonably simple to engineer and requires only a single fibre, bidirectional, downlead from which light can be coupled to the sensor using a single lens.

In principle a single, narrow-band, light source emitting continuous illumination would be adequate for this system, the intensity of the light reflected from the sensor head being dependent upon the pressure. However, in practice, this approach would suffer from two major potential sources of error:

(i) Crosstalk between the transmitted and returning signals, caused by light reflected from optical components local to the transmitter being superimposed on that reflected from the sensor head.

(ii) Spurious variations in the sensor return signal, due to changes in the transmitted intensity and microbending of the optical fibre downlead.

The first of these effects, crosstalk between the transmitted and received signals, can be minimised by modulating the light source and using phase sensitive detection to achieve "range gating" of signals. With reference to figure 3, Tx and Rx represent the transmitted and received signals from the light source. If Tx is modulated at a frequency which is one quarter of the reciprocal of the time taken for light to travel to the sensor head and back, there will be a $\pi/2$ phase error between the signals received directly from the source and from the sensor head. When these are multiplied by a suitable reference waveform derived from the modulation signal, and then low pass filtered, the desired signal will be retrieved as a voltage level proportional to the light intensity returning from the sensor, whereas the other will be strongly attenuated. (Figure 3 shows this procedure applied to the signal received from the sensor head and also to the transmitted light signal. (As will be explained both of the signals need to be measured).

Errors due to changes in the transmitted optical power and bending-induced attenuation in the fibre can be largely eliminated by using a two wavelength characterisation approach. Two narrow-band light sources (light emitting diodes in the present work) are used simultaneously and, after demultiplexing, the ratio of the returning signal and the transmitted intensity is calculated for each of the two wavelengths (i.e. I_1/T_1 and I_2/T_2). Both of these ratios are independent of source intensity changes. The ratio $(I_1/T_1)/(I_2/T_2)$ is then calculated by a further division to yield a result which is largely immune to downlead microbending effects, and is only dependent on the applied pressure. Note that each channel employs phase sensitive detection.

Both of the above techniques were used in our sensor system providing the advantages of range gating and dual wavelength referencing.

Description of Prototype Equipment

The sensor head

As shown in figure 4, the sensor head consisted of two separate units: the etalon and lens support, and the fibre support. The Fabry-Perot etalon was supported by a silicone rubber seal allowing the external pressure to bear directly on the flexing silica substrate.

A graded index rod (Grinrod) lens was used to collimate the incident illumination and also to re-launch the reflected light into the single optical fibre downlead. The grinrod lens was particularly suitable for this application due to its small size, convenient cylindrical geometry and compatibility with optical fibre. It was bonded into the support, which was held in position by a compressed 'O' ring seal.

The construction of the etalon is shown in figure 5. It comprised two plane, parallel silica substrates bonded into a gold-plated invar collar with waterproof cement. The spacer was formed by vacuum deposition of a silica annulus onto the surface of one of the reflectors. (The thick silica substrate is effectively rigid and acts as a positional reference. Pressure acts on the thin plate, causing it to flex). A buffer zone, also produced by vacuum deposition, limited the allowable distortion of the flexing mirror under over-pressure conditions. (It is unlikely that the substrate would fracture in the absence of the buffer zone, but damage to the reflecting surfaces could occur if the mirrors were forced into contact; the buffer zone prevents this).

Ideally, the mirror separation should be chosen such that I_1, I_2 (the intensities of the reflected light from the two sources) and I_1/I_2 all change over as large a range as possible, whilst remaining single valued functions of pressure. This is achieved by arranging the spacer and flexing mirror thicknesses such that the mirror separation changes from approximately 1.3 to 1.2um over the required pressure range as shown in figure 6. The choice of mirror separation is, of course, influenced by the wavelengths of the light sources; in figure 6, wavelengths of 780nm and 890nm are assumed.

The mirror reflectivities are not critical, but the chosen value was a compromise between maximizing the reflected intensity and maintaining a reasonable width to the Fabry-Perot reflection minima, which determined the available operating range and, indirectly, the temperature sensitivity. 20% reflectivity was used, as this was considered to be a reasonable compromise.

Optical system

A schematic diagram of the system is shown in figure 7. The intensity- modulated optical power, provided by two light emitting diodes (LEDs) with optical fibre pigtails, was launched into the 1.1km fibre cable via a commercial fibre-tailed wavelength-division multiplexer. The four signals which were necessary to determine the pressure, (i.e., the sensor return signals I_1 and I_2 and the transmitted light intensities T_1 and T_2) were monitored by separate silicon P.I.N. diodes via a bidirectional fibre coupler and two wavelength-division demultiplexers (all fully encapsulated commercially available fibre-tailed devices).
Multimode 100/140um graded index fibre was used throughout, except for the LED pigtails which were of 50/125um fibre.

The operating wavelengths chosen for the LEDs were determined by the following factors:

(a) The need to minimize crosstalk in the wavelength-division multiplexers. For practical purposes this crosstalk normally decreases as the wavelength separation of the two sources increases.

(b) The power of available devices and the requirement for low and similar attenuation of the optical fibre at the two wavelengths.

Bearing all these factors in mind, the operating wavelengths selected were 780 and 890nm.

Electronics

The electronics comprised four separate units:
(i) Master oscillator
(ii) LED drive circuit
(iii) Phase sensitive detection reference signal generator
(iv) Signal processing unit.

The master oscillator controlled the LED drivers and the PSD reference signal generator, in order to guarantee that the frequencies and phases of the reference signals A, B, C and D were locked to those of the transmitted illumination.

The two light emitting diodes were driven simultaneously by a 1:1 mark space ratio square wave, the frequency of which was determined by the length of the optical fibre downlead. The modulation frequency of the transmitted light must be such that the phase difference at the silion pin diodes, between light returning from the sensor head and that routed directly from the LEDs, is $\pi/2$ radians. In these experiments, which utilized 1.1 km downlead, the necessary modulation frequency to achieve this was 23kHz.
The four signals monitored by the silicon pin diodes (two sensor return signals and two transmitted light signals) were independently amplified and phase sensitively detected to yield four voltage levels. These were proportional to the intensities of the two wavelengths transmitted to, and received from, the sensor head. These levels were then ratioed, as shown in figure 7 to give a result which was essentially independent of changes in the transmitted optical power and (to a first order) downlead microbending effects.

Experimental Results

With the end seal in place, air pressure was applied to the sensor head via the brass tube (figure 4). A capacitive pressure transducer was used to monitor the applied pressure and to provide a calibration reference. The sensor output, as well as the intensities of the two reflected signals, was measured as a function of pressure, and the results are plotted in figure 8. It can be seen from figures 6 and 8 that the experimental response has the form expected and, for this etalon, the range of pressure for an inambiguous output was approximately 0 to 13 psi. The range is simply determined by the thickness of the flexing substrate in the Fabry Perot, and can therefore be tailored for most applications.

In order to assess the immunity of the system to bending-induced attenuation in the optical fibre downlead, bends of different radii were formed, and the corresponding sensor output and the intensities of the received signals were monitored. For these measurements the sensor was unpressurized. The dependence of sensor output on bending-induced loss is shown in figure 9, from which it can be seen that the use of two wavelengths provides an improvement factor of approximately ten over an unreferenced system. Measurements of the received optical powers have shown that the remaining sensitivity to bending is not due to inaccuracy in the dividers, and it is therefore attributed to the wavelength dependence of the bending-induced attenuation.

Conclusion

A simple and compact fibre optic pressure sensor, based on a Fabry Perot etalon, has been demonstrated. A two-wavelength technique was used to eliminate sensitivity to bending of the sensor downlead, and range gating prevented errors due to unwanted optical reflections. The reflective configuration used is attractive for remote sensor location, a single multimode fibre downlead can be used. The pressure range demonstrated was 0 to 13 psi, but it is a simple matter to construct etalons for other ranges by changing the thickness of the flexing substrate appropriately.

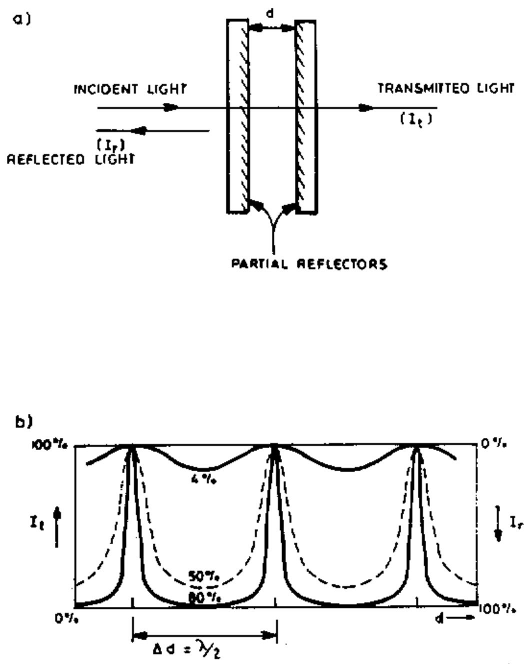

Figure 1 Fabry-Perot etalon: a) Schematic; b) Form of reflected and transmitted intensities.

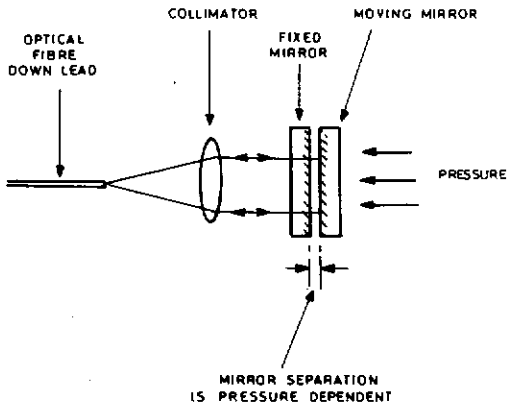

Figure 2   Schematic diagram of reflecting Fabry-Perot sensor head.

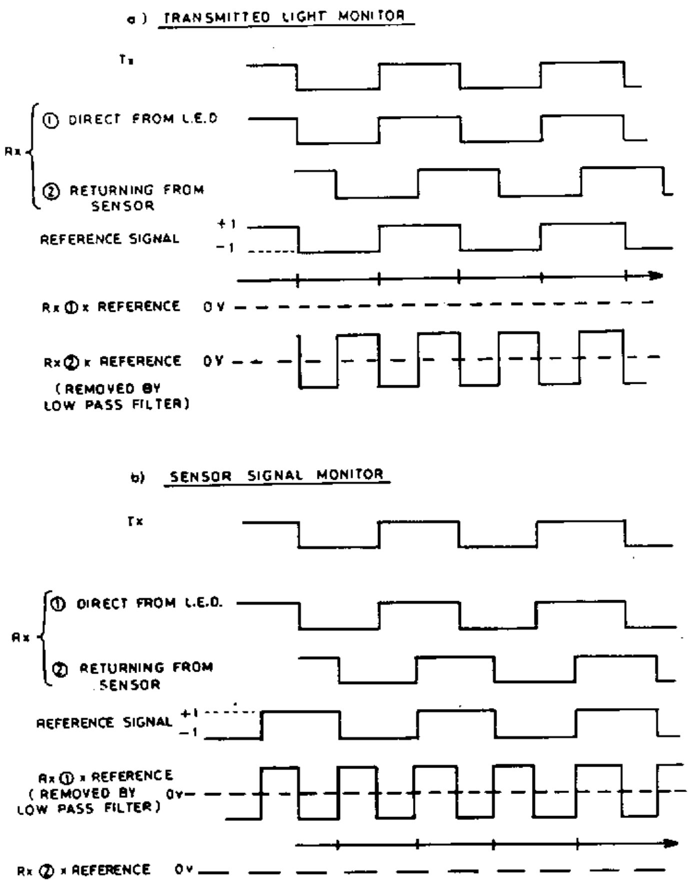

Figure 3   Principle of phase sensitive detection.

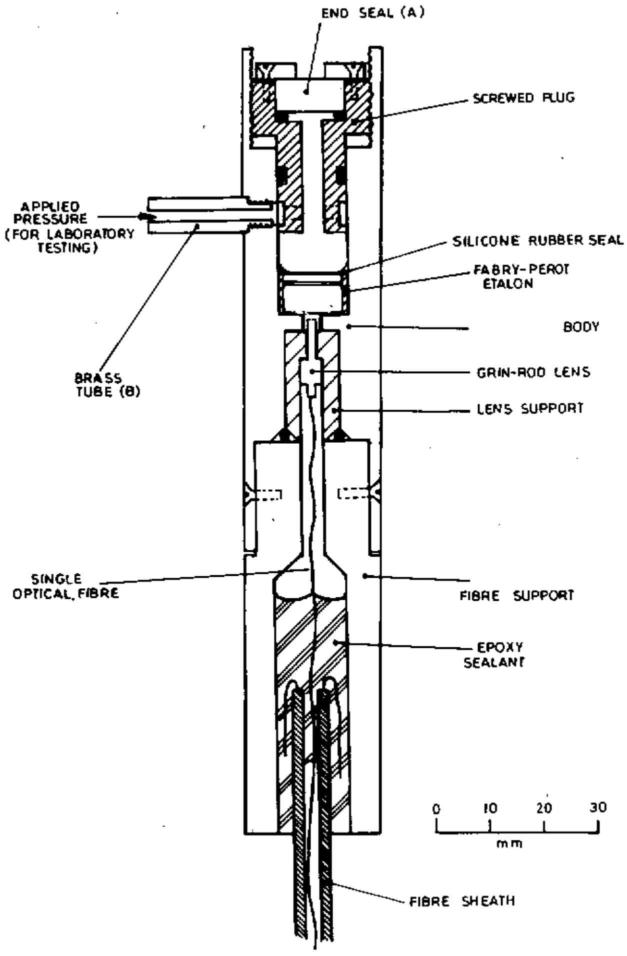

Figure 4 Fabry-Perot pressure sensor head.

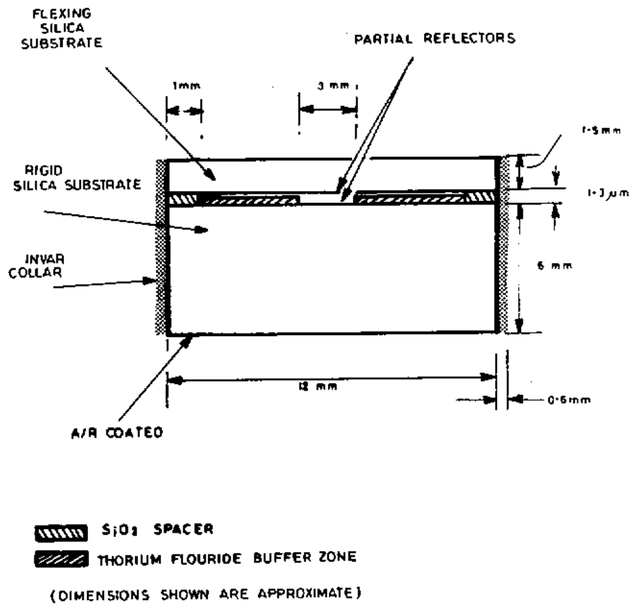

Figure 5 Fabry-Perot etalon.

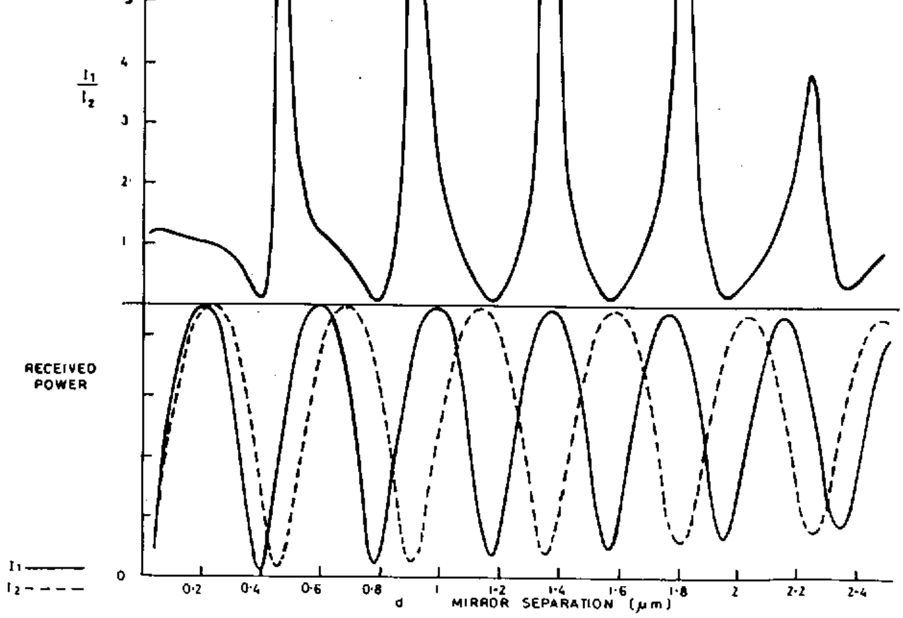

Figure 6 Fabry-Perot sensor output (schematic).

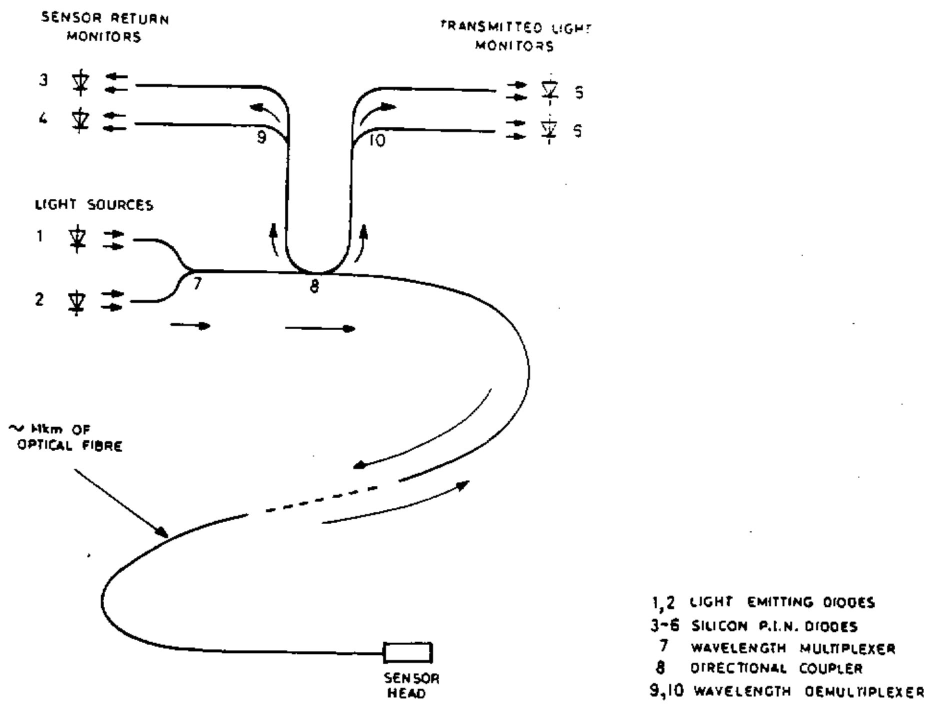

Figure 7 Pressure sensor optical system.

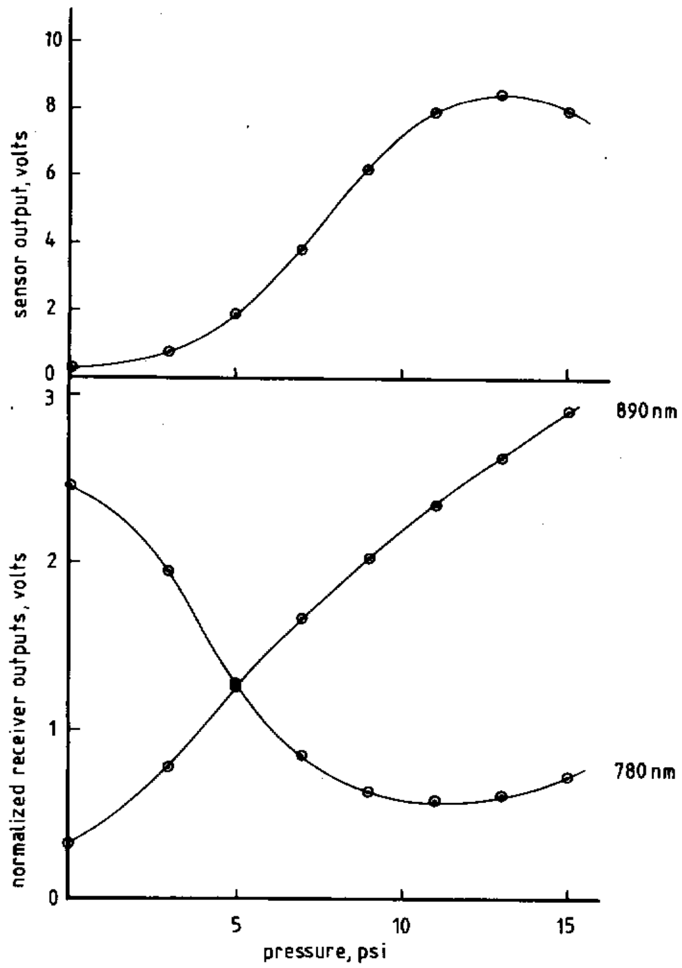

Figure 8 Measured sensor outputs.

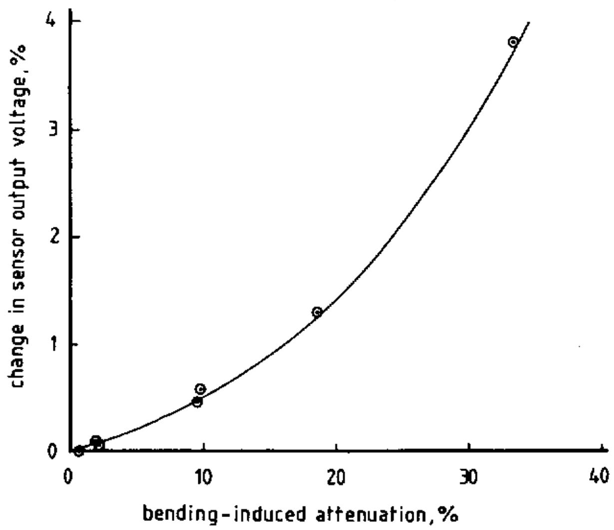

Figure 9 Effect of bending-induced fibre attenuation on sensor output.